REVISTA Mundi
Engenharia, Tecnologia e Gestão
INSTITUTO FEDERAL

BRAIN THERMAL AND ELECTRICAL PROPERTIES ESTIMATION USING EXPERIMENTAL DATA FROM DEEP BRAIN STIMULATION LEAD

ESTIMAÇÃO DE PROPRIEDADES TÉRMICAS E ELÉTRICAS DO CÉREBRO UTILIZANDO DADOS EXPERIMENTAIS PROVENIENTES DE UMA SONDA DE ESTIMULAÇÃO CEREBRAL PROFUNDA

Lucas Correia da Silva Jardim[1]

Luiz Alberto da Silva Abreu[2]

Diego Campos Knupp[3]

Antônio José da Silva Neto[4]

Abstract: Deep Brain Stimulation (DBS) is a well-established neurosurgery that alleviates the symptoms of several movement disorders and other brain related conditions. It works by placing a small lead containing electrodes inside the patient's brain and using them to electrically stimulate that area. Although this procedure is very common, little is known about its physiological effects on the brain and, on top of that, injuries caused from burning have been reported. The present work intends to formulate and solve a bioheat transfer model of the brain containing a DBS lead and, furthermore, to use this solution for solving an inverse problem of determining the thermal and electrical conductivities of the brain tissue using measurements supposedly obtained with a sensor inside the DBS lead.The results revealed that it is possible to estimate the both parameters especially when the measurements uncertainties are relatively small.

***Keywords*:** Deep brain stimulation. Bioheat transfer. Inverse problem. Parameter estimation. Electrical heating.

[1]Mestre em Modelagem Computacional, Universidade do Estado do Rio de Janeiro, ljardim@iprj.uerj.br.
[2]Doutor em Engenharia Mecânica, Universidade do Estado do Rio de Janeiro, luiz.abreu@iprj.uerj.br.
[3]Doutor em Engenharia Mecânica, Universidade do Estado do Rio de Janeiro, diegoknupp@iprj.uerj.br.
[4]Doutor em Engenharia Mecânica, Universidade do Estado do Rio de Janeiro, ajsneto@iprj.uerj.br.

Resumo: A Estimulação Cerebral Profunda (DBS) é uma neurocirurgia já bem estabelecida e que alivia os sintomas de vários distúrbios do movimento e outras condições relacionadas ao cérebro. Seu funcionamento se dá através da colocação de uma pequena sonda contendo eletrodos dentro do cérebro e os utiliza para estimular eletricamente uma área específica. Embora seja um procedimento já difundido, pouco se sabe sobre seus efeitos fisiológicos no cérebro e, além disso, relatos de lesões devido ao aumento de temperatura já foram reportados. O presente trabalho visa formular e resolver um modelo de bio-transferência de calor no cérebro contendo um eletrodo DBS e, além disso, usar esta solução para resolver um problema inverso de estimação das condutividades térmicas e elétricas do tecido cerebral usando medidas supostamente obtidas com um sensor dentro da sonda de DBS. Os resultados revelaram que é possível estimar os dois parâmetros, especialmente quando as incertezas das medições são relativamente pequenas.

***Palavras-chave*:** Estimulação cerebral profunda. Bio transferência de calor. Problema inverso. Estimação de parâmetro. Aquecimento elétrico.

1 INTRODUCTION

The surgery known as Deep Brain Stimulation (DBS) is a neurosurgical procedure where an electrical stimulator is implanted in a specific brain region in order to reduce the symptoms of several tremor diseases. Starting at the end of the decade of 1980, DBS has become highly accepted as treatment for Parkinson's disease (OBESO *et al.*, 2001), dystonia (VIDAILHET *et al.*, 2005), epilepsy (HODAIE *et al.*, 2002) and others (KRINGELBACH *et al.*, 2007). To this day, new investigations are still discovering and increasing the collection of diseases that is possible to treat with DBS.

The Figure (1) shows a simplified representation of the DBS system and its implementation inside the patient's head. An electrical signal with specific frequency is generated by the circuit on the neurostimulator, which is a pacemaker-like device installed subcutaneously near the clavicle of the patient. This signal is delivered to the lead via an extension cord, a subcutaneous wire. The thin, insulated and coiled wires inside the lead carry this signal to the electrodes on its ending. Then, these electrodes delivers the stimulation to the targeted area of the brain (COFFEY, 2009; KRINGELBACH *et al.*, 2007).

Figure 1: Representation of the DBS system with detail on the lead inside the brain.

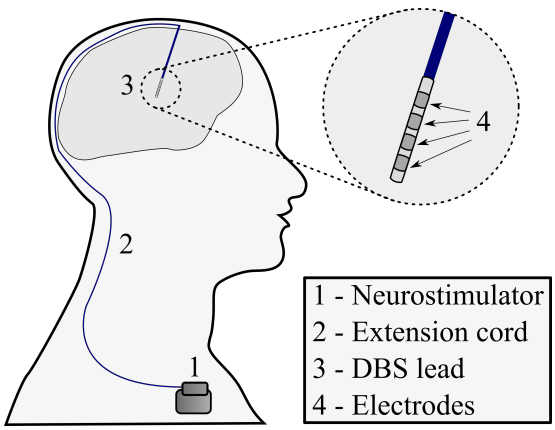

Source: The authors, 2020.

Despite its use being largely spread worldwide and having a well-tolerated surgical procedure (ASHKAN *et al.*, 2017), little is known about DBS's physiological effects on the brain and, on top of that, some of the most common injuries are related to possible internal burns from thermal coupling with other equipment, such as magnetic resonance imaging (ELWASSIF *et al.*, 2012). Although less common, there are injuries reported in the literature which are related to internal burn during normal operation (PATTERSON; MARK; BRETT, 2007).

In this context, the present work intends to formulate and solve a bioheat model of the

brain with a DBS lead. The Penne's model (PENNES, 1948) is coupled with the Laplace equation of electrical field yielding two partial differential equations. This theoretical approach to solve the electrical heating due to DBS's activity was originally introduced in (ELWASSIF *et al.*, 2006). Furthermore, the present work aims to use this solution as a direct problem of an inverse analysis to obtain estimates of thermal and electrical conductivities of the brain. This information can be of great value to avoid injuries due to temperature increase. Results show that positioning a sensor inside the DBS lead can generate useful experimental data for physicians to characterize the patient brain, given that the sensor is accurate enough.

2 FORMULATION AND SOLUTION OF THE DBS HEATING PROBLEM

To understand the heating process caused by the electrical stimulation of the brain, two Medtronic® DBS leads are studied: Model 3387 and Model 3389. These are cylindrical leads with 1.27 mm of diameter and, in each one, there are four electrodes with 1.5 mm of length. The main difference between them is the electrodes spacing, with distances of 1.5 mm on the Model 3387 and 0.5 mm on Model 3389, as schematically presented in Fig. 2

Figure 2: Schematic representation of Medtronic's Model 3389 and Model 3387 showing the geometrical configuration of the electrodes.

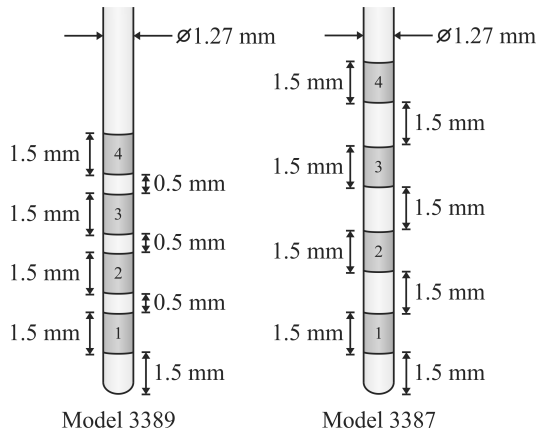

Source: Adapted from (MEDTRONIC; INC, 2002).

Considering the axisymmetric plane defined by the length of the lead and the radius of a cylindrical coordinates system, as illustrated in Fig. 3. This plane has boundaries ranging from $r = R_1$ to $r = R_2$, where R_1 is the radius of the lead and R_2 a sufficient long distance, and from $z = 0$ to $z = H$, where H is a sufficient long height. Also in Fig. 3, the term z^{exp} represents the height where the sensor is located.

Figure 3: Schematic representation of the computational axisymmetric domain.

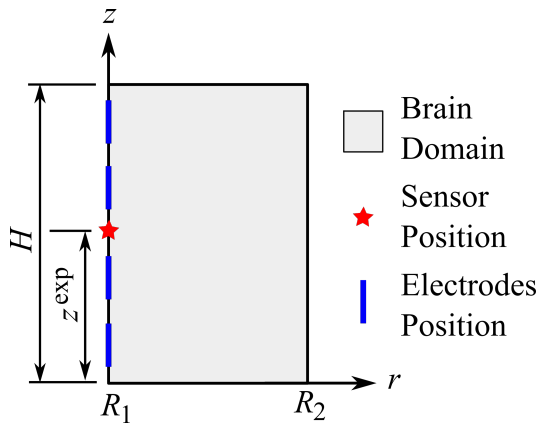

Source: The authors, 2020.

To describe how temperature increases on the brain with the electrical stimulator, phenomena such as blood perfusion and metabolic heat generation must be considered. So the model proposed by (PENNES, 1948) and (PERL, 1962) is used herein. The Joule heating due to the DBS electrical activity is caused by the current flowing from one electrode to another. It can be added to the bioheat model by terms of the electrical potential $V(r, z)$, which is calculated by the Laplace equation. So the bioheat equation, in axisymmetrical cylindrical coordinates, is given by

$$\frac{1}{r}\frac{\partial}{\partial r}\left(k\, r\frac{\partial T}{\partial r}\right) + \frac{\partial}{\partial z}\left(k\frac{\partial T}{\partial z}\right) - \rho_b\, \omega_b\, c_b(T - T_b) + Q_m + \sigma|\Delta V|^2 = \rho\, c_p\frac{\partial T}{\partial t} \tag{1}$$

$$\left.\frac{\partial T}{\partial r}\right|_{r=R_1} = 0 \tag{2}$$

$$T(r, z, t) = T_a \text{ at } r = R_2,\ z = 0,\ z = H \tag{3}$$

where, for the brain tissue, k is the thermal conductivity, ρ is the specific mass, c_p is the specific heat, σ is the electrical conductivity and Q_m the metabolic heat generation. The temperature T_a is the initial brain temperature when there is no electrical heating. The parameters related to the blood perfusion are ω_b, ρ_b, c_b and T_b, which are the blood perfusion parameter, the specific mass, the specific heat and the temperature, respectively, for the blood in the brain. As previously mentioned, $V(r, z)$ is the electrical potential, which can be directly calculated by the Laplace equation in cylindrical coordinates, given by

$$\frac{1}{r}\frac{\partial}{\partial r}\left(\sigma\, r\frac{\partial V}{\partial r}\right)+\sigma\frac{\partial^2 V}{\partial z^2}=0 \tag{4}$$

$$\frac{\partial v}{\partial \mathbf{n}}=0 \text{ at } r=R_2,\ z=0,\ z=h \tag{5}$$

$$V(R_1,z)=f(z) \tag{6}$$

The problem given by Eq. (1) to Eq. (6) is solved with the built-in routine *NDSolve* of the Wolfram Mathematica 10.0 system (WOLFRAM, 2005), which is used here with an automatic absolute and relative error control. The chosen method of solution is the Finite Elements Method (FEM) as a sub-routine of *NDSolve*.

3 INVERSE PROBLEM FORMULATION AND SOLUTION

Acquiring experimental temperature data inside the brain can be challenging and complicated in terms of technology and two main difficulties can be encountered when dealing with the DBS heating process: the small size of the lead and the also small variation of temperature due to normal DBS operation. This work proposes the use of a sensor inside the lead positioned at halfway distance between electrodes 2 and 3, therefore, the objective of this work is to evaluate if is possible estimate the parameters accurately assuming that the sensor is in the position shown in the Fig. 3.

Since experimental data are not available, they are simulated by adding random noise to the solution of the direct problem given by Eq. (1) to Eq. (6). These errors are drawn from a normal distribution centered in zero and are calculated with the expression

$$T_i^{\text{exp}}=T(R_1,\ z^{\text{exp}},\ t_i^{\text{exp}})+e_i,\ \text{with } e_i\sim \text{N}(0,\ \epsilon^2),\ i=1,\ 2,...,\ N_d \tag{7}$$

where N_d is the total number of experimental data, z^{exp} is the height corresponding to the position of the temperature sensor, $\mathbf{t}^{\text{exp}}$ is the vector containing time instants when such data is acquired and ϵ is the standard deviation of the experimental data. The reader should note that the exact temperature is calculated at $r=R_1$ and $z=z^{\text{exp}}=H/2$, i.e., as already mentioned, at the lead-brain interface and in the middle of the four electrodes.

The thermal and electrical conductivity, k and σ respectively, are here considered unknowns and, not only that, their prior information can be modeled as a normal distribution in order to obtain the inverse problem formulation as a Maximum a Posteriori (MAP) objective function. This approach allows us to obtain single point estimates for the unknowns and

approximations for the confidence intervals (KNUPP *et al.*, 2016). So, the MAP objective function can be written as

$$Q(\mathbf{Z}) = \left[\mathbf{T}^{\text{exp}} - \mathbf{T}^{\text{calc}}(\mathbf{Z})\right]^T \mathbf{W}^{-1} \left[\mathbf{T}^{\text{exp}} - \mathbf{T}^{\text{calc}}(\mathbf{Z})\right] + \left(\mu_{\text{pr}} - \mathbf{Z}\right)^T \mathbf{V}^{-1} \left(\mu_{\text{pr}} - \mathbf{Z}\right) \quad (8)$$

where $\mathbf{Z}$ is the vector of unknown estimatives, $\mathbf{T}^{\text{exp}}$ the vector containing the experimental data, $\mathbf{T}^{\text{calc}}$ is the calculated temperatures with $\mathbf{Z}$, $\mathbf{W}$ is the covariance matrix, $\mathbf{V}$ is the priori covariance matrix and μ_{pr} is the mean of the prior information. To minimize this objective function, the Gauss-Newton iterative procedure is applied and it can be formulated as (BECK; ARNOLD, 1977)

$$\mathbf{Z}^{n+1} = \mathbf{Z}^n + \left[\left(\mathbf{J}^T\right)^n \mathbf{W}^{-1}\mathbf{J} + \mathbf{V}^{-1}\right]^{-1} \times \left[\left(\mathbf{J}^T\right)^n \mathbf{W}^{-1} \left[\mathbf{T}^{\text{exp}} - \mathbf{T}^{\text{calc}}(\mathbf{Z})\right] + \mathbf{V}^{-1} \left(\mu_{\text{pr}} - \mathbf{Z}\right)\right] \quad (9)$$

where $\mathbf{J}$ is the Jacobian matrix, which have its elements defined by

$$J_{ij} = \frac{\partial T_i^{\text{calc}}}{\partial Z_j}, \; i = 1, 2, ..., N_d \text{ and } j = 1, 2, ..., N_u \quad (10)$$

with N_u being the number of unknowns and N_d was already defined as the total number of experimental data.

To obtain approximations of the standard deviation of the posterior distribution for each parameter, one can use the following expression

$$\sigma_{z_i} = \sqrt{\left[\left(\mathbf{J}^T\mathbf{W}^{-1}\mathbf{J} + \mathbf{V}^{-1}\right)^{-1}\right]_{i,i}} \quad (11)$$

The expression given by Eq. (11) is an approximation when dealing with non-linear inverse problems. Even with the prior information and the experimental noise modeled as a normal distribution, it is not possible to guarantee that the posterior distribution is, in fact, also modeled by a normal distribution (SCHWAAB *et al.*, 2008).

Table 1: Exact values of the parameters of the direct problem.

Parameter	Value	Dimension	Observation
T_b	36.7	[°C]	Blood temperature
σ	0.35	[S/m]	Electrical conductivity
k	0.527	[W/m.K]	Thermal conductivity
H	50.0	[mm]	Height of the domain
R_1	0.635	[mm]	First radius of the domain
R_2	20.0	[mm]	Second radius of the domain
Q_m	9132.0	[W/m^3]	Internal metabolic heat generation
c_p	3650	[J/kgK]	Specific heat of the brain tissue
ρ	1040	[kg/m^3]	Specific mass of the brain
ω_b	0.008	[ml/s.cm^3]	Blood perfusion
ρ_b	1057	[kg/m^3]	Specific mass of the blood
c_b	3600	[J/kg.K]	Specific heat of the blood

4 RESULTS AND DISCUSSION

4.1 Direct Problem Solution and Results

In order to obtain the solution of the direct problem given by Eq. (1) to Eq. (6), several parameters related to the physiology of the brain must be known. The exact values of these parameters can be readily found in the literature and, in this work, the ones from (ELWASSIF *et al.*, 2006) are used. Table (1) summarizes all the values used for the solution of the direct problem and, later on, this solution is used to generate the experimental data.

The boundary condition proposed in Eq. (6) must be set as a step function where the DBS electrical potential is applied only at the position of active electrodes. In this work, the V_{rms} of the DBS high setting operation mode is used due to its higher capacity of generating heat. This setting generates an electrical signal of 10 V, 185 pps and 210 ms yielding a V_{rms} of 1.561 V (ELWASSIF *et al.*, 2006).

The solution obtained with these parameters is displayed in Fig. 4, where Fig. 4a represents the temperature distribution and Fig. 4b the electrical potential distribution. These results are obtained in $t = 1000$ s, which, from our results, can be reasonably considered as steady state. The pair of active electrodes selected are 1 and 4 – see Fig. 2 – and the DBS lead type is the Model 3389.

In Fig. 5(a), it is possible to see the magnitude of the temperature increase, which is approximately 0.65 °C, for that configuration. This result shows that, in order to identify this temperature variation, the sensor placed inside the DBS lead and in the middle of the electrodes must have a precision of 0.05 °C, which is considerably small for today's technology

but somewhat achievable with a thermistor.

The Finite Elements mesh is composed by 2786 triangular elements, generated with the option *"MaxCellMeasure"* included in the *NDSolve* routine. The same mesh is used for both the electrical and the temperature problem. This approach can benefit from the use of different mesh for each problem, as it is possible to see that the electrical problem got some unwanted oscillations in its solution.

Figure 4: Solution of both the temperature and the electrical problem for Model 3389 with activity on electrodes 1 and 4.

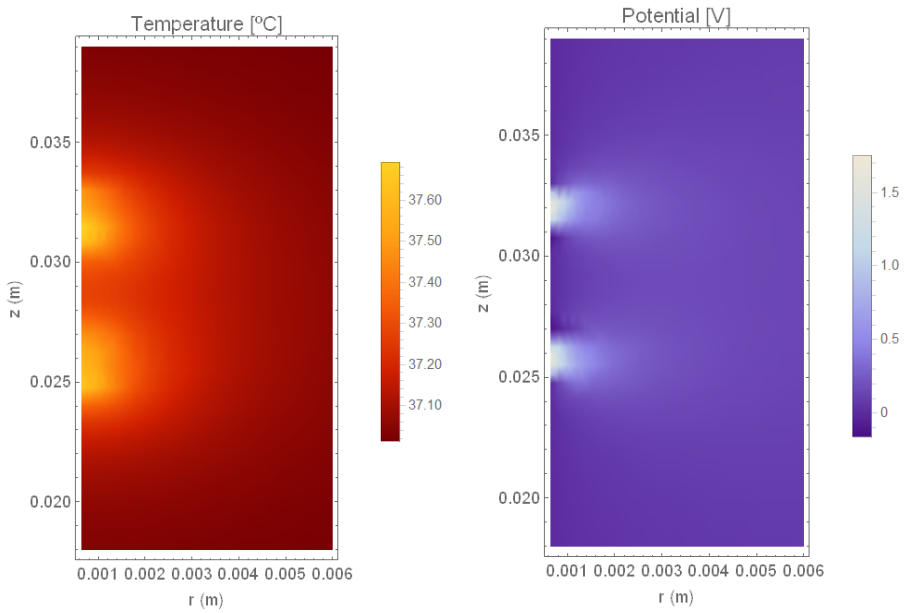

(a) Temperature profile (b) Electrical potential

Source: The authors, 2020.

4.2 Inverse Problem Solution and Results

To acquire experimental data, the vector containing the instants of time $\mathbf{t}^{\text{exp}}$ range from 1 s to 61 s with fixed intervals of $\Delta t = 1$ s, which generates $N_d = 61$ experimental data. Using $\epsilon = 0.05$ ºC and $\epsilon = 0.025$ ºC in Eq. (7), the experimental noise can be added in order to simulate real data. This level of error is relatively low when dealing with temperature information, but considering the maximum amplitude variation of temperature obtained in the problem, this is a fundamental condition to obtain a solution within a reasonable confidence region. Figure (5) shows the exact solution with their respective experimental data obtained for both noise levels. Observe how the experimental data spread along on the plot range of 0.4 ºC. In this context, noise level of $\epsilon = 0.05$ ºC generates more realistic measurements of temperature.

Figure 5: Experimental data along with exact solution for Model 3389 with activity on electrodes 1 and 4 for two noise levels: $\epsilon = 0.05$ ºC and $\epsilon = 0.025$ ºC in Eq. (7), respectively.

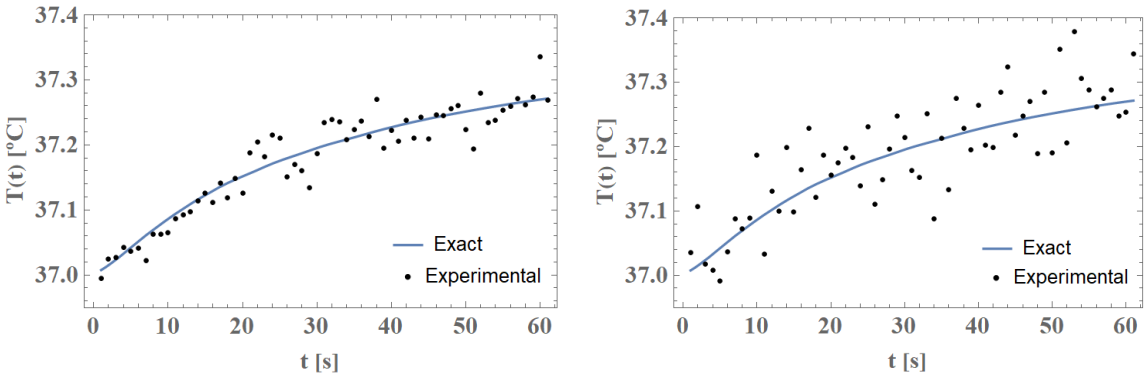

(a) $\epsilon = 0.05$ ºC (b) $\epsilon = 0.025$ ºC

Source: The authors, 2020.

To solve the inverse problem using the MAP approach, a prior information of the unknown parameters must be set. In this work it is used arbitrary information for both the thermal and electrical conductivities. Their mean values are both set as 0.5 W/m.K and 0.5 S/m, respectively, and their standard deviation as 0.25 W/m.K and 0.25 S/m, which represents a considerable large interval centered in an expected value.

For the iterative method described in Eq. (9), the approach used is to fix the number of iterations in five steps. The main goal is to have a solution influenced mainly by the MAP formulation and to have a somewhat predictable computational time. The derivative in Eq. (10) is obtained with a centered finite difference formula using an interval of 1% for each parameter exact value.

The results displayed on Tab. (2) and (3) are the ones obtained for DBS lead Model 3389 with the pairs of electrodes 1-2 and 1-4 actives, respectively. Tables (4) and (5) presents the results for the Model 3387, with the same pairs of electrodes mentioned. These two pairs of electrodes are the only ones tested: 1-2 and 1-4. Since the sensor is positioned in the middle of the four electrodes, it is expected that pairs 2-3 will render the best results due to increased temperature reading, therefore we omitted the results for this pair.

Six independent experiments were performed for each configuration of lead type, pairs of electrode actives and noise level, meaning that the experimental data are different for each one. Since the optimization method used is deterministic and the starting point is the same for every scenario, there is no need to perform multiple executions with the same experimental data.

The terms k^* and σ^* on Tab. (2) to (5) represent the mean value obtained for the thermal and electrical conductivity, respectively. The standard deviation is presented below of each

parameter estimation inside parentheses. As explained in Section 3, this posterior normal distribution is a linear approximation, so this standard deviation displayed correspond to this approximation deviation.

Firstly, the reader must notice how much more accurate are the estimatives for the electrical conductivity σ in comparison to the thermal conductivity k. This indicates a higher sensitivity of the electrical problem, meaning that changes in σ are more noticeable on the temperature profile resultant than changes in k. In every configuration, the averages for the standard deviations of the electrical conductivity is smaller than its thermal conductivity counterpart.

Although the thermal conductivity generated small intervals with the most sensible set up (Model 3389, electrodes 1 and 2 and noise levels of $\epsilon = 0.25$ ^{o}C), the mean value of of $k = 0.4022$ W/m.K estimated in Experiment 2 W/m K is considerably far from its exact value of $k = 0.5270$ W/m.K. In spite of that poor result, the averages for the mean values of the six experiments presented in Tab. (2) are acceptable when compared to the exact value, indicating that these average standard deviations are somewhat expectable.

The results for lead type Model 3387, in Tab. (4) and (5), are supposed to have less precise intervals since the temperature variation is smaller than the ones from Model 3389 and, indeed, they do for the parameter k. When comparing the average standard deviations this becomes clear: thermal conductivity estimatives enlarges its standard deviation more than electrical conductivity when going from Model 3389 to Model 3387. The reader can grasp this observation by comparing results from Tabs. (2) with (4) and Tabs. (3) with (5).

5 CONCLUSIONS

The DBS electrical activity inside the brain causes a temperature increase by Joule effect. In this work, this heating process was modeled as an axis-symmetrical problem in order to obtain the temperature distribution around the brain with active electrodes. This model is then used to formulate a practical inverse problem where, with one temperature sensor inside the DBS's lead, experimental temperature data are acquired and used to estimate the thermal and electrical conductivities of the brain tissue. This inverse problem was formulated and solved using the Maximum a Posteriori method, which resulted in approximation for the posteriori distribution. This approach showed that it is possible to estimate those parameters simultaneously with only one sensor inside the lead, but the accuracy of this sensor must be considerably high and its positioning inside the lead must be as close to active electrodes as possible.

Table 2: Results obtained using DBS lead Model 3389 with electrode pair 1-2 active and experimental noise levels of $\epsilon = 0.025$ ºC and $\epsilon = 0.050$ ºC.

Model 3389 - Electrodes 1 and 2				
ϵ	0.025 ºC		0.050 ºC	
u_i	k^* (Std. Dev.)	σ^* (Std. Dev.)	k^* (Std. Dev.)	σ^* (Std. Dev.)
Exp. #1	0.4477 (0.0722)	0.3135 (0.0378)	0.5970 (0.1449)	0.3925 (0.0729)
Exp. #2	0.4022 (0.0675)	0.2873 (0.0356)	0.6164 (0.1523)	0.3950 (0.0745)
Exp. #3	0.5440 (0.0998)	0.3547 (0.0495)	0.4915 (0.1347)	0.3276 (0.0676)
Exp. #4	0.5281 (0.0572)	0.3513 (0.0274)	0.4480 (0.1037)	0.3135 (0.0501)
Exp. #5	0.5862 (0.0681)	0.3746 (0.0314)	0.4516 (0.0214)	0.3132 (0.0081)
Exp. #6	0.5957 (0.0724)	0.3820 (0.0333)	0.5918 (0.1275)	0.3725 (0.0577)
Avg.	**0.5222 (0.0728)**	**0.3439 (0.0358)**	**0.5327 (0.1140)**	**0.3523 (0.0551)**
Dim.	[W/m.K]	[S/m]	[W/m.K]	[S/m]

Table 3: Results obtained using DBS lead Model 3389 with electrode pair 1-4 active and experimental noise levels of $\epsilon = 0.025$ ºC and $\epsilon = 0.050$ ºC.

Model 3389 - Electrodes 1 and 4				
ϵ	0.025 ºC		0.050 ºC	
u_i	k^* (Std. Dev.)	σ^* (Std. Dev.)	k^* (Std. Dev.)	σ^* (Std. Dev.)
Exp. #1	0.4951 (0.0715)	0.3402 (0.0205)	0.5585 (0.1310)	0.3727 (0.0388)
Exp. #2	0.5858 (0.0509)	0.3799 (0.0253)	0.5469 (0.1270)	0.3634 (0.0387
Exp. #3	0.5806 (0.0824)	0.3631 (0.0235)	0.4385 (0.1192)	0.3183 (0.0338)
Exp. #4	0.5212 (0.0688)	0.3581 (0.0174)	0.4457 (0.1133)	0.3247 (0.0269)
Exp. #5	0.4815 (0.0533)	0.3467 (0.0292)	0.5730 (0.1223)	0.3547 (0.0322)
Exp. #6	0.4710 (0.0644)	0.3342 (0.0154)	0.4598 (0.0661)	0.3123 (0.0191)
Avg.	**0.5225 (0.0652)**	**0.3537 (0.0218)**	**0.5037 (0.1131)**	**0.3410 (0.0324)**
Dim.	[W/m.K]	[S/m]	[W/m.K]	[S/m]

Table 4: Results obtained using DBS lead Model 3387 with electrode pair 1-2 active and experimental noise levels of $\epsilon = 0.025$ ºC and $\epsilon = 0.050$ ºC.

Model 3387 - Electrodes 1 and 2				
ϵ	0.025 ºC		0.050 ºC	
u_i	k^* (Std. Dev.)	σ^* (Std. Dev.)	k^* (Std. Dev.)	σ^* (Std. Dev.)
Exp. #1	0.6568 (0.1189)	0.4001 (0.0489)	0.6377 (0.1774)	0.3980 (0.0742)
Exp. #2	0.5726 (0.1075)	0.3747 (0.0466)	0.3670 (0.1396)	0.2765 (0.0654)
Exp. #3	0.5854 (0.1108)	0.3726 (0.0468)	0.5848 (0.1778)	0.3547 (0.0713)
Exp. #4	0.4545 (0.0475)	0.3181 (0.0239)	0.6834 (0.1579	0.3996 (0.0755)
Exp. #5	0.4477 (0.0994)	0.3163 (0.0454)	0.5294 (0.0394)	0.3574 (0.0183)
Exp. #6	0.5644 (0.1169)	0.3685 (0.0502)	0.5142 (0.0541)	0.3491 (0.0264)
Avg.	**0.5249 (0.1001)**	**0.3583 (0.1169)**	**0.5527 (0.1243)**	**0.3558 (0.0551)**
Dim.	[W/m.K]	[S/m]	[W/m.K]	[S/m]

Table 5: Results obtained using DBS lead Model 3387 with electrode pair 1-4 active and experimental noise levels of $\epsilon = 0.025$ ºC and $\epsilon = 0.050$ ºC.

Model 3387 - Electrodes 1 and 4				
ϵ	0.025 ºC		0.050 ºC	
u_i	k^* (Std. Dev.)	σ^* (Std. Dev.)	k^* (Std. Dev.)	σ^* (Std. Dev.)
Exp. #1	0.4347 (0.1601)	0.3369 (0.0158)	0.6140 (0.2152)	0.3448 (0.0361)
Exp. #2	0.4338 (0.1501)	0.3710 (0.0128)	0.4686 (0.1576)	0.3729 (0.0291)
Exp. #3	0.5184 (0.1528)	0.3622 (0.0189)	0.4276 (0.1279)	0.4041 (0.0386)
Exp. #4	0.4556 (0.1434)	0.3714 (0.0176)	0.6050 (0.2161)	0.3599 (0.0376)
Exp. #5	0.4140 (0.1303)	0.3587 (0.0146)	0.2931 (0.1935)	0.3191 (0.0321)
Exp. #6	0.7910 (0.1874)	0.3686 (0.0279)	0.6119 (0.2175)	0.3550 (0.0378)
Avg.	**0.5079 (0.1540)**	**0.3614 (0.0179)**	**0.5033 (0.1879)**	**0.3593 (0.0352)**
Dim.	[W/m.K]	[S/m]	[W/m.K]	[S/m]

ACKNOWLEDGMENTS

The authors acknowledge the financial support provided by CAPES – Coordenação de Aperfeiçoamento de Pessoal de Nível Superior (Finance Code 001), CNPq – Conselho Nacional de Desenvolvimento Científico e Tecnológico, and FAPERJ – Fundação Carlos Chagas Filho de Amparo à Pesquisa do Estado do Rio de Janeiro.

REFERENCES

ASHKAN, K. *et al.* Insights into the mechanisms of deep brain stimulation. *Nature Reviews Neurology*, v. 13, n. 9, p. 548, 2017.

BECK, J.; ARNOLD, K. *Parameter Estimation in Engineering and Science*. New York: Wiley Interscience, 1977.

COFFEY, R. J. Deep brain stimulation devices: a brief technical history and review. *Artificial Organs*, v. 33, n. 3, p. 208–220, 2009.

ELWASSIF, M. M. *et al.* Temperature control at dbs electrodes using a heat sink: experimentally validated fem model of dbs lead architecture. *Journal of Neural Engineering*, v. 9, n. 4, 2012.

ELWASSIF, M. M. *et al.* Bio-heat transfer model of deep brain stimulation-induced temperature changes. *Journal of Neural Engineering*, v. 3, n. 4, p. 306, 2006.

HODAIE, M. *et al.* Chronic anterior thalamus stimulation for intractable epilepsy. *Epilepsia*, v. 43, n. 6, p. 603–608, 2002.

KNUPP, D. C. *et al.* Inverse analysis of a new anomalous diffusion model employing maximum likelihood and bayesian estimation. *Mathematical Modeling and Computational Intelligence in Engineering Applications*, Springer, Cham, p. 89–104, 2016.

KRINGELBACH, M. L. *et al.* Translational principles of deep brain stimulation. *Nature Reviews Neuroscience*, v. 8, n. 8, p. 603–608, 2007.

MEDTRONIC; INC. *DBS Lead Kit for Deep Brain Stimulation, Model 3387/3389, Implant Manual*. Minneapolis, MN, US: [s.n.], 2002.

OBESO, J. A. *et al.* Deep-brain stimulation of the subthalamic nucleus or the pars interna of the globus pallidus in parkinson's disease. *New England Journal of Medicine*, v. 345, n. 13, p. 956–963, 2001.

PATTERSON, T.; MARK, M. S.; BRETT, L. N. Mechanisms of electrode induced injury. part 2: clinical experience. *American Journal of Electroneurodiagnostic Technology*, v. 47, n. 2, p. 93–113, 2007.

PENNES, H. H. Analysis of tissue and arterial blood temperatures in the resting human forearm. *Journal of Applied Physiology*, v. 1, n. 2, p. 93–122, 1948.

PERL, W. Heat and matter distribution in body tissues and the determination of tissue blood flow by local clearance methods. *Journal of Theoretical Biology*, v. 2, n. 3, p. 201–235, 1962.

SCHWAAB, M. *et al.* Nonlinear parameter estimation through particle swarm optimization. *Chemical Engineering Science*, v. 63, n. 6, p. 375–395, 2008.

VIDAILHET, M. *et al.* Bilateral deep-brain stimulation of the globus pallidus in primary generalized dystonia. *New England Journal of Medicine*, v. 352, n. 5, p. 459–467, 2005.

WOLFRAM, S. *The Mathematica Book*. Cambridge: Wolfram Media, 2005.

Edição especial - XXII ENMC (Encontro Nacional de Modelagem Computacional) e X ECTM (Encontro de Ciência e Tecnologia dos Materiais)

Enviado em: 01 jul. 2020

Aceito em: 10 ago. 2020

Editor responsável: Rafael Alves Bonfim de Queiroz